SPHERICAL REGRESSION IN QUALITY ASSURANCE

G.R. Chapman and P.T. Kim

IIQP Research Report
RR-92-01

January 1992

SPHERICAL REGRESSION IN

QUALITY ASSURANCE

G.R. Chapman
Maximus Inc.
56 Old Colony Trail
Guelph, Ontario N1G 4A9

Peter T. Kim
Department of Statistics and Actuarial Science
University of Guelph
Guelph, Ontario N1G 2W1

ABSTRACT

In this paper, we display the role that spherical regression can play in the geometric quality assurance of any finely engineered product, such as automobile parts. A review is given of spherical regression, with particular reference to diagnostics. Finally, results are presented of a numerical simulation, that display the power of these diagnostics.

Key words and phrases: Diagnostics; least squares; quality assurance; rotations; spherical regression.

1. INTRODUCTION

In many industrial settings, *e.g.*, the automobile industry, it is necessary to assess the geometric integrity of component parts. Traditionally, the procurer of the part has issued geometric specifications and tolerances against which the supplier's product is tested. A physical mould is constructed made of wood, plastic, *etc.*, and an attempt is made to clamp the part into place. Tolerance is checked with a feeler gauge. Such methods are expensive, time consuming and of limited accuracy.

More recently, Computer Assisted Design (CAD) has allowed the designer to create a prototype part in the form of a computer image. It is then possible to generate a data file that takes the place of the traditional blueprint, or specification. The surface of the image of the part is covered with a fine mesh and both the spatial coordinates, and the coordinates of the unit normal vector are generated, at each mesh point. The resulting file is called the CAD file, and the quality assurance problem is now to test whether a sample part conforms to the CAD file, to within specified tolerances.

The device used to check the geometric integrity of a part is a Coordinate Measuring Machine (CMM). The part is held firmly in position, and points on the surface of the part are touched with the CMM probe. The spatial coordinates of the points that are touched are accurately measured and recorded. It is important to note that the coordinates so obtained are with respect to an axis system internal to the CMM. On the other hand vectors in the CAD file are expressed relative to some coordinate system determined by the software that created the CAD file. The problem is therefore to construct a transformation between the two coordinate systems. The CMM measurements could then be transformed and checked against the CAD data file.

Constructing the transformation is more difficult than might at first appear. Since the CAD data consists of only a finite number of points, the mesh points mentioned above, an arbitrarily chosen point on the part will in most instances not correspond to any CAD data point. Even if such a point did appear in the CAD data, there is no practical way

of identifying it. Thus it is not possible to construct a transformation by simply matching CMM points to CAD data points.

A Euclidean transformation is required, *i.e.*,

$$x \rightarrow Ax + T, \tag{1.1}$$

where x, T are 3-vectors, and A is a 3×3 rotation matrix. The purpose of this paper is to display a method of estimating the rotation, followed by outlining diagnostic procedures that assess the fit so that a statistical determination of whether or not the part is defective can be made.

A word about what is meant by defective should be made precise. If we think of a part as simply a three dimensional object, then assuming that this part has distinct features (see below), one can describe this part as consisting of planar regions as well as the dimensions; length, width, height, *etc.* In this paper we consider only the rotational part of the transformation. Consequently, this will allow a methodology for analyzing defective planar regions only. To analyze the dimensions as well, one also has to estimate the translation. The latter issue will not be discussed in the current paper and will be detailed in a subsequent paper.

The rotation is constructed as follows. First CMM readings are used to estimate directional features of the part. By directional features, we mean *e.g.*, unit vectors normal to small planar regions on the part, or a unit vector indicating the direction of some line, such as a trim-edge. Counterparts to these directions can be found in, or calculated from, the CAD data file. Then, the methods of spherical regression, see Chang (1986), are applied to construct the rotation (plus possible reflection) that causes the least squares fit between these CMM directional data and their CAD data counterparts. Rivest (1989) gives diagnostics for spherical regression, and these can be used to check the integrity of those aspects of the part represented by the directional data. Indeed, using these diagnostics for just the rotation parameter determines that a part is defective in the sense that a collection

of planar regions in the part do not align with one another in the way demanded by the CAD data and that it is possible to determine which plane is out of alignment.

At this point we wish to note that the technology employed in this paper is most useful when the part in question has distinct features such as; flat regions, edges, points, *etc.* If the part in question consists solely of smooth curves and surfaces, for example the wing of an aircraft, or an automobile fender, the techniques outlined in this paper may not readily be applicable. We note however, that if one is willing to assume local flatness in some radius of each point relative to some scale, then the techniques outlined in this paper can be used.

We now give a summary of what is to follow. In Section 2, we discuss measurement errors induced by CMM, along with a method of estimating directional features of the part, from CMM data. Section 3 is a review of spherical regression along with relevant diagnostics given by the penetrating paper of Rivest (1989). In Section 4, we present some simulations with respect to estimating measurement errors induced by the CMM, followed by two examples illustrating the methodology. The final Section 5, present the results of a numerical simulation, that displays the power of the diagnostics in situations similar to those encountered in practice. We include an Appendix which outlines how data is simulated.

2. MEASUREMENT OF FEATURES

Given a part to be tested it is usually possible to find various directional features that can be both identified in the CAD data file, and estimated using CMM measurements. There are two types of directional features: unit vectors indicating the direction of a line in the part, and unit vectors normal to planar regions in the part. While there are many ways the former can arise, in practice they are much less used than the latter. For this reason, we restrict our discussion to the planar situation, which is adequate for the purposes of this paper.

The procedure is therefore, to identify n planar regions on the surface of the part, $n \geq 3$. The unit normal vectors to these planes in the CAD data coordinate system, denoted by $v_1, \ldots, v_n$, can be found by looking in the appropriate general region of the CAD data file, for a collection of mesh points with a common normal. The corresponding normals in the CMM coordinate system $(u_1, \ldots, u_n)$ are then estimated as described below, and spherical regression can be used to estimate the orthogonal transformation required to best fit the transformed $(u_1, \ldots, u_n)$ to $(v_1, \ldots, v_n)$, in a least square sense.

2.1. CMM Resolution

Before using CMM measurements to estimate the normal vector to a plane, it is necessary to consider the nature of CMM measurement error. Typically, a CMM display consists of the three spatial coordinates it is measuring, expressed in *mm*. The three readings change independently of one another, however, only certain coordinate values are allowed for certain decimal places. Assuming that the CMM always returns the allowed coordinate value that is nearest to the true value, then the errors on the coordinates are independent of one another, and are dependent on what is called the *resolution* of the CMM, which we denote by ϵ. The unit of measurement of the resolution is known as, *micron*, where one micron is 10^{-3} *mm*. Thus in the situation where $\epsilon = 5$, which is the situation usually encountered in practice, the third decimal place can only take values of 0 or 5 so that the spatial coordinates have errors of plus or minus 2.5 microns. The resolution varies from one make and model type of CMM to another, and in the simulation study of Section 4 we consider $\epsilon = 5$, 10, 25 and 50 microns.

2.2. Estimating Directional Features

In view of this error structure, given points $x_1, \ldots, x_m$ measured on the surface of a plane, the normal vector to the plane, u, is estimated by minimizing

$$\sum_{i=1}^{m} d(x_i; u^t x = c)^2, \tag{2.1}$$

where $d(x_i; u^t x = c)$ denotes the perpendicular distance of x_i from the plane $u^t x = c$ and B^t denotes the transpose of some matrix or vector B. This problem has been of interest to crystallographers, and a number of solutions have been presented, see Schomaker *et. al.* (1959), Blow (1960), Scheringer (1971). A simple solution is to use the method of principal component analysis. Put

$$\bar{x} = m^{-1} \sum_{i=1}^{m} x_i, \quad D = \sum_{i=1}^{m} (x_i - \bar{x})(x_i - \bar{x})^t. \tag{2.2}$$

The smallest eigenvalue of D gives the minimum value of (2.1), and the corresponding unit eigenvector, $\hat{u}$, is the estimate of u. To ensure that $\hat{u}$ points in the right direction, *i.e.*, is an outward normal, a point x_{m+1} can be read by the CMM, above the surface of the plane. The sign of $\hat{u}$ is adjusted so that

$$\hat{u}^t (x_{m+1} - \bar{x}) > 0. \tag{2.3}$$

The accuracy of the estimate $\hat{u}$ depends not only on the resolution of the CMM, but also on the number m of points on the plane, and how widely spread these points are. The greater the area covered by these points the better, but in practice one has to restrict this area to remain confident that the points are in fact planar. In Section 5, we simulate a situation that often occurs in practice: planar normals are estimated using six points measured around a circle of radius 1 *cm*, and judged by eye to be evenly spread around the circle.

3. SPHERICAL REGRESSION AND DIAGNOSTICS

Spherical regression is a procedure which statistically estimates an orientation parameter based on spherical data. The problem was originally solved by MacKenzie (1957), and the solution has been developed by Moran (1976), Stephens (1979) and Chang (1986). Rivest (1989) developed diagnostic procedures for the concentrated Fisher-von Mises distribution. Kim (1991) examined spherical regression in a decision theoretic framework

and obtained Bayes estimators for the unknown rotation under general conditions. Applications of spherical regression have included: crystallography, see MacKenzie (1957); the motion of tectonic plates, see Chang (1986, 1989) and Rivest (1989); and, vector cardiogram orientation, see Prentice (1989). To the best of our knowledge, this is the first application of spherical regression techniques, to an industrial setting, in particular, to quality assurance.

3.1. Estimation of Rotation

Let u be a random vector distributed on the two dimensional unit sphere S^2 having density $f(u^tAv)$ with respect to the invariant measure on S^2. Here $v \epsilon S^2$ is fixed and known, and the unknown parameter of interest A, is a 3×3 rotation matrix. Thus the collection of all 3×3 rotation matrices $SO(3)$, is the parameter space.

Given a random sample $u_1, \ldots, u_n$, and the corresponding set $v_1, \ldots, v_n$ of design points, the objective in spherical regression is to estimate the unknown rotation A so as to,

$$\min_{A \epsilon SO(3)} n^{-1} \sum_{i=1}^{n} \|u_i - Av_i\|^2, \tag{3.1}$$

where $\|\cdot\|$ denotes the usual Euclidean distance. This is equivalent to,

$$\max_{A \epsilon SO(3)} n^{-1} \sum_{i=1}^{n} u_i^t A v_i. \tag{3.2}$$

Following MacKenzie (1957), we have,

$$n^{-1} \sum_{i=1}^{n} u_i^t A v_i = n^{-1} \mathrm{tr} U^t A V = n^{-1} \mathrm{tr} A V U^t, \tag{3.3}$$

where $U = (u_1, \ldots, u_n)$, $V = (v_1, \ldots, v_n)$ and $\mathrm{tr}M$ denotes the trace of some square matrix M. Write,

$$n^{-1} V U^t = O_1 \Lambda O_2^t, \tag{3.4}$$

where O_1, O_2 are rotation matrices, and $\Lambda = \text{diag}(\lambda_1, \lambda_2, |\lambda_3|)$, with $\lambda_1 \geq \lambda_2 \geq |\lambda_3| \geq 0$. This is sometimes called a *modified* singular value decomposition, see Stephens (1979). From (3.3),

$$n^{-1}\text{tr}AVU^t = \text{tr}O_2^t AO_1\Lambda. \tag{3.5}$$

As A ranges over $SO(3)$, so too does $O_2^t AO_1$. Since elements of $SO(3)$ have entries of absolute value less than or equal to unity, (3.5) is maximized when

$$O_2^t AO_1 = I, \quad \text{or} \quad A = O_2 O_1^t. \tag{3.6}$$

We denote $A_{ls} = O_2 O_1^t$ and call it the *least squares* estimator of A. We note that if $\lambda_1 > \lambda_2 > |\lambda_3| > 0$, which would occur for large n, then A_{ls} is unique. Chang (1986) showed that if $A \epsilon SO(3)$ is the true parameter, then

$$A_{ls} \to A, \tag{3.7}$$

as $n \to \infty$, provided $n^{-1}\sum_{i=1}^n v_i v_i^t$ converges to some positive definite matrix as $n \to \infty$. In Figure 3.1, we illustrate the procedure involved.

3.2. Diagnostics

Suppose the distribution of the $u's$ is that of a Fisher-von Mises distribution,

$$f(u^t Av) = c(\kappa)^{-1}\exp\{\kappa u^t Av\}, \tag{3.8}$$

where $c(\kappa) = \kappa^{-1}\text{sinh}\kappa$. Here $\kappa > 0$ in addition to $A \epsilon SO(3)$, is a parameter of interest.

Define

$$W_i = \begin{bmatrix} 0 & -v_{i3} & v_{i2} \\ v_{i3} & 0 & -v_{i1} \\ -v_{i2} & v_{i1} & 0 \end{bmatrix}, \tag{3.9}$$

where $v_i = (v_{i1}, v_{i2}, v_{i3})^t$, $i = 1, \ldots, n$. It was shown by Rivest (1989) that

$$2n\kappa(1 - r) \to_d \chi^2_{2n-3}, \tag{3.10}$$

as $\kappa \to \infty$ for each fixed n, provided $\sum_{i=1}^{n} W_i^t W_i$ is nonsingular, where "$\to_d$" means convergence in distribution and

$$r = n^{-1} \sum_{i=1}^{n} u_i^t A_{ls} v_i. \tag{3.11}$$

We note that the approximation is $o_p(\kappa^{-1/2})$, hence the approximation is very good, see Rivest (1989, 309).

For each fixed v_i, let $v_{i(1)}$ and $v_{i(2)}$ be mutually orthogonal unit vectors perpendicular to v_i for each $i = 1, \ldots, n$. Thus $(v_i, v_{i(1)}, v_{i(2)})$ form an orthonormal basis for $\mathbf{R}^3$. Define

$$e_i = (v_{i(1)}, v_{i(2)})^t A_{ls}^t u_i, \tag{3.12}$$

for $i = 1, \ldots, n$ as the *residuals* of spherical regression. We note that the motivation for defining (3.12) comes from ordinary linear regression. Indeed, residuals in the latter can be thought of as the orthogonal projection of the data onto the complementary subspace spanned by the design matrix. Notice that the situation is similar in (3.12) in the spherical regression context. This insight was first pointed out by Rivest (1989).

We can then form the statistic

$$t_i^2 = \frac{(n - 5/2) e_i^t \Sigma_i^{-1} e_i}{2n(1 - r) - e_i^t \Sigma_i^{-1} e_i}, \tag{3.13}$$

where

$$\Sigma_i = (v_{i(2)}, -v_{i(1)})^t [I - n^{-1}(I - S)^{-1}](v_{i(2)}, -v_{i(1)}), \tag{3.14}$$

for $i = 1, \ldots, n$, where $S = n^{-1} \sum_{i=1}^{n} v_i v_i^t$. We once again note that (3.13) is motivated by ordinary linear regression, in that (3.13) is an adaptation of Cook's test for outliers, see Rivest (1989). We have that,

$$t_i^2 \to_d F_{2,2n-5}, \tag{3.15}$$

for each $i = 1, \ldots, n$ as $\kappa \to \infty$.

The parameter, $\kappa > 0$, records the amount of concentration of the data u, around $A^t v$, with greater concentration being determined by large values of κ. Consequently, (3.10)

can be used to form the test, $H_0 : \kappa \geq \kappa_0$ against $H_1 : \kappa < \kappa_0$, where the κ_0 would represent the amount of allowable tolerance. With respect to the latter, a variety of ways of obtaining κ_0 could be used, depending on the situation involved along with engineering practices. One way of obtaining κ_0 would be to base it on the CMM resolution, so that the amount of allowable tolerance is that which is induced by measurement error in the CMM. In fact this is how it is done in the simulations of Section 4, where we will further discuss this point. By (3.10), a rejection region of approximate size α would be given by,

$$2n\kappa_0(1-r) > \chi^2_{2n-3,\alpha}, \tag{3.16}$$

where $\chi^2_{\nu,\alpha}$ is the upper α^{th} percentile of a chi square distribution with ν degrees of freedom.

Another aspect involved in quality testing would be to find out whether the i^{th} data point is an outlier, thus indicating that point to be defective, particularly if the above H_0 is rejected but the data is still concentrated. Thus (3.13) could be used along with (3.15). Indeed, let the null hypothesis be, that the i^{th} data point be regular, *i.e.*, not defective. Then an approximate size α rejection region would be,

$$t_i^2 > F_{2,2n-5,\alpha}, \tag{3.17}$$

where $F_{\nu,\mu,\alpha}$ denotes the upper α^{th} percentile of an F distribution with ν and μ degrees of freedom. We once again note that this procedure is similar to Cook's procedure for testing for outliers in ordinary linear regression, see Rivest (1989).

3.3. Further Remarks

We remark that although the diagnostics are developed when the errors are distributed according to the Fisher-Von Mises distribution, it is felt that all of the above results should generalize to a wider class of distributions. This would follow because for very concentrated errors, one essentially is approximating the curvilinear surface S^2, linearly, *i.e.*, by it's tangent plane. Since κ is controlling the amount of variability around the

preferred direction, when κ is large one can essentially ignore the curvy part and just rely on the linear part.

We remark that the theory of spherical regression, as outlined here, has been developed for the parameter space $SO(3)$. This is because the applications for which the theory has been developed have required that a rotation matrix be estimated. It is interesting to note that in the quality assurance problem, the parameter space $O(3)$, of all orthogonal 3×3 matrices, is more appropriate. This is because CAD data files can be expressed in either left or right hand coordinate systems and there is often no way of knowing which has been used, when testing a part. An orthogonal matrix will accommodate both situations.

In the $O(3)$ parameter space case, the solution to the problem,

$$\min_{A \epsilon O(3)} \sum_{i=1}^{n} \|u_i - Av_i\|^2, \tag{3.18}$$

is largely the same as that presented above. The only difference is that in (3.4) we allow O_1, O_2 to be orthogonal matrices. This is then the usual (rather than modified) singular value decomposition: see *e.g.*, Golub and Van Loan (1983). As before,

$$A_{ls} = O_2 O_1^t, \tag{3.19}$$

and the two coordinate systems (CAD and CMM) are compatible if $\det(A_{ls}) = 1$, incompatible if $\det(A_{ls}) = -1$. If the latter turns out to be the case, one can make appropriate modifications to the CAD data so that the parameter space would once more be $SO(3)$.

4. SPHERICAL REGRESSION AND DIAGNOSTICS: APPLICATIONS

This section discusses the practical aspects behind using the methodology outlined in the previous section. The examples that will be discussed, are simulated data, where the simulations attempt to capture the type of situation normally encountered in practice. The way in which the data is simulated, is outlined in the Appendix. In the following, we will outline how κ_0 can be chosen, followed by two illustrations involving data.

4.1. Estimating κ_0

Define,

$$s = 1 - r, \tag{4.1}$$

It follows from (3.10) that, s is distributed as approximately, $(2n\kappa)^{-1}\chi^2_{2n-3}$, when $\kappa > 0$ is large. Thus, if we observe a random sample $s_1, \ldots, s_N$, then by the usual derivations, the maximum likelihood estimator is,

$$\hat{\kappa} = \frac{2n-3}{2n\bar{s}}, \tag{4.2}$$

where $\bar{s}$ denotes the sample mean. Further,

$$Var(\hat{\kappa}) \approx \frac{2n-3}{2Nn^2\bar{s}^2}. \tag{4.3}$$

Thus by comparing (4.2) with (4.3), the amount of variability in $\hat{\kappa}$ is very small when κ and N are large.

Therefore, to get a good estimate of the magnitude of the error induced by CMM resolution, samples (of s) of size 1000 are generated for a geometrically perfect part, for variety of scenarios obtained by varying n, and ϵ (the resolution of the CMM). Values of n are considered between $n = 3$ (the minimum number required to uniquely determine A_{ls}) and $n = 10$ (about the largest number commonly used in practice). It is found that for fixed ϵ, $\hat{\kappa}$ did not vary significantly with n. Table 4.1 gives a summary of the simulations. We emphasize that the usual CMM resolution encountered in practice is 5 microns, thus a fair estimate for κ_0 is approximately 36,000,000. The interpretation of the latter is simply the error likely to be encountered due exclusively to measurement inaccuracy of the CMM.

4.2. Examples

We present below two examples of situations that could arise in practice and outline how the diagnostics are to be used. The discussion will begin with the normal vectors of both the CAD and CMM data so that we are assuming that the manufactured part has

been measured by a CMM with the normal vectors computed as outlined in Section 2.2. In both situations, $n = 10$, $\epsilon = 5$ with the rows representing the spatial normals obtained by CAD and CMM.

Example 1

CAD			CMM		
0.000000	-0.500000	0.866025	-0.700302	-0.658766	0.274960
-0.433013	0.250000	0.866025	-0.604233	0.025961	0.796385
0.433013	0.250000	0.866025	-0.011011	-0.604895	0.796229
-0.206651	-0.213993	0.954726	-0.736907	-0.409955	0.537498
0.057891	-0.010208	0.9998271	-0.471301	-0.522491	0.710548
-0.287907	-0.030644	0.957168	-0.697914	-0.261490	0.666738
0.074708	-0.493985	0.866255	-0.646279	-0.710247	0.279056
-0.004769	-0.147224	0.989092	-0.581310	-0.540085	0.608594
-0.058984	-0.014313	0.998156	-0.553530	-0.439435	0.707461
0.045825	-0.488085	0.871592	-0.665685	-0.688735	0.287241

By (3.6), the least squares estimator is

$$A_{ls} = \begin{bmatrix} 0.685065 & 0.523684 & -0.506399 \\ -0.728482 & 0.492350 & -0.476347 \\ -0.000130 & 0.695231 & 0.718786 \end{bmatrix}. \tag{4.4}$$

In this example, we have,

$$2n\kappa_0(1-r) = 15.429, \tag{4.5}$$

where $\kappa_0 = 35,745,557$. Thus the $p-$value of (4.5), in comparison with a chisquare random variable with 17 degrees of freedom, is 0.565. Thus based on (3.16), we cannot reject the null hypothesis that the manufactured part is not defective.

We also present the $p-$values associated with each datum using (3.5).

Test for outliers

i^{th} datum	1	2	3	4	5	6	7	8	9	10
t_i^2	0.426	0.089	0.012	5.848	1.786	0.964	0.700	0.215	0.906	0.826
$p-$value	0.660	0.915	0.988	0.013	0.202	0.404	0.512	0.809	0.425	0.457

The i^{th} datum refers to the i^{th} row of the data. Notice that all the $p-$values are insignificant at 0.01, although the 4^{th} datum is significant at 0.05. Thus if there is a suspicion that the manufactured part is defective, it would be with regard to that planar region. We note however, that (3.16) is not significant, so it is likely that datum is not an outlier.

Example 2

CAD			CMM		
0.000000	-.500000	0.866025	-0.700229	-0.658418	0.275980
-0.433013	0.250000	0.866025	-0.604435	0.026290	0.796221
0.433013	0.250000	0.866025	-0.011082	-0.604670	0.796399
-0.206651	-0.213993	0.954726	-0.737032	-0.409668	0.5357547
0.057891	-0.010208	0.998271	-0.471198	-0.522807	0.717384
-0.287907	-0.030644	0.957168	-0.697980	-0.261241	0.666766
0.074708	-0.493985	0.866255	-0.646241	-0.710077	0.279578
-0.004769	-0.147224	0.989092	-0.581317	-0.540115	0.608561
-0.058984	-0.014313	0.998156	-0.553386	-0.439561	0.707496
0.045825	-0.488085	0.871592	-0.665560	-0.688920	0.287087

Again by (3.6), the least squares estimator is

$$A_{ls} = \begin{bmatrix} 0.685124 & 0.523623 & -0.506383 \\ -0.728426 & 0.492591 & -0.476182 \\ 0.000099 & 0.695106 & 0.718907 \end{bmatrix}. \tag{4.6}$$

In this example, we have,

$$2n\kappa_0(1-r) = 49.880, \tag{4.7}$$

where $\kappa_0 = 35,745,557$. Thus the $p-$value of (4.7), is 0.001, so that based on (3.16), we can reject the null hypothesis and conclude that the manufactured part is defective.

Again, we present the $p-$values associated with each datum using (3.5). We note that for this example, the latter is more meaningful since the overall test is declaring the part to be defective.

Test for outliers

i^{th} datum	1	2	3	4	5	6	7	8	9	10
t_i^2	27.722	0.254	0.082	0.201	0.656	0.041	0.492	0.280	0.303	0.411
$p-$value	0.001	0.779	0.921	0.820	0.533	0.960	0.621	0.759	0.743	0.670

Notice that all except the 1^{th} datum, the $p-$values are insignificant at any reasonable value. Thus given (3.16) classifies the manufactured part as being defective, one would suspect that by (3.17), the defect is in the 1^{th} planar region.

Indeed, the tests did a very reasonable job in declaring the part to be defective and locating the source of error. In example 1, the only aberration in the data, came from measurement error. In example 2, we had distorted the first planar region by 0.001 radians through one of the axis.

5. FURTHER SIMULATIONS

In this section, we report some of the other simulations performed.

5.1. Diagnostics with One Displaced Normal

For $n = 3$ and 10, one normal is arbitrarily chosen and displaced by an angle ϕ. Data is generated for 100 trials of the part, for a given CMM resolution ϵ, the idea being to simulate 100 tests of the same defective part. The statistics r and t_i^2 are calculated for each trial. The value $\phi = 0$ is included, to simulate a geometrically perfect part. We would also like to point out, that the latter could serve as a way of testing the calibration of the CMM.

The criterion used for rejecting the part, *i.e.*, declaring it defective, is, following (3.16),

$$2n\hat{\kappa}(1-r) > \chi^2_{2n-3,0.05}, \tag{5.1}$$

where $\hat{\kappa}$ is the maximum likelihood estimate of κ based on the sample drawn from the perfect part and represents the uncertainty due to the resolution of the CMM. Tables 5.1a, 5.1b display the results for $n = 3$ and $n = 10$ normals, respectively. From these tables one can ascertain the machine resolution required to detect a given angular displacement, for example, a CMM with 5 micron resolution is adequate for detecting displacements of 0.001 radians, whereas a 10 micron resolution machine is not.

To attempt to identify which normal is displaced, we use (3.17) and identify the i^{th} normal as displaced if

$$t_i^2 > F_{2,2n-5,0.05}. \tag{5.2}$$

Table 5.2 shows the frequency with which the displaced normal is correctly identified as being displaced, in 100 trials. The ability to detect the displaced normal increases with n, as can be seen by comparing parts (a) and (b) of Table 5.2. For $n = 3$ the only situation considered that adequately allows identification of the displaced normal is the extreme situation where $\phi = 0.01$ radians and $\epsilon = 5$ microns. A comparison of Tables 5.1b, 5.2b indicates that when $n = 10$ the ability to identify the specific normal displaced, *via* (5.2), slightly exceeds the ability to declare the part defective overall, *via* (5.1).

It is also possible for (5.2) to indicate that one of the true (undisplaced) normals is displaced. Table 5.3 indicates the frequency of this occurrence. It should be noted when reading Table 5.3 that there are 9 true normals when $n = 10$ and only 2 when $n = 3$.

5.2. Diagnostics with More than One Displaced Normal

In practice, situations are likely to be encountered where more than one normal is displaced. Since it is impractical to simulate all possibilities, we will illustrate the methodology with a few simple examples.

The simulation of the previous section is repeated but with three normals displaced rather than one. All three displacements are through the same angle ϕ, but about different arbitrary axes. In the $n = 3$ case all normals are displaced and for $n = 10$ the three to be displaced are chosen randomly from among the ten.

Results of applying criterion (5.1) are given in Table 5.4. On comparison with Table 5.1, the improved detection capability that one would anticipate, is apparent.

Criterion (5.2) is less effective in this situation. In no circumstances are all three displaced normals simultaneously correctly identified. Table 5.5 shows the frequency of detection of one or two of the displaced normals, in 100 trials.

We conclude by remarking that it is possible to construct examples where three normals are displaced by rotation through an angle ϕ about selected axes, and (5.2) fails to detect any of the three displaced normals at any time. Further analyses as well as simulations are currently being done.

5. DISCUSSION

Traditional methods of assessing the geometric integrity of any finely engineered product requires the use of fixtures. The fit is then tested with a feeler gauge. Fixtures are expensive to construct and transport and the degree of accuracy obtained may be insufficient, depending on the tolerance specified by the procurer of the part.

Through CAD technology one can design a perfect part on a computer screen. Furthermore a manufactured part can be spatially measured by a CMM after which the quality assurance is to see if the CAD and CMM data conform. We have shown how techniques of spherical regression as well as associated diagnostics are then important tools to statistically assess whether or not the manufactured part meets the prespecifications within some level of tolerance.

We note that this is the first application of spherical regression techniques to an industrial setting and expect the ramifications to be an important contribution of statistics to quality assurance.

APPENDIX

The data for the simulations and the examples are created in the following way:

- n planar regions are identified on a part ($n \geq 3$);
- the corresponding unit normal vectors $v_1, \ldots, v_n$ are located in the CAD data file;
- six points are measured with a CMM on the surface of each of the n planes. Each set of six points is suppose to have been spaced around a circle of radius 1 cm.

The steps taken in the simulation are:

Step 1, let

$$v_0 = (0, 0, 1), \quad \theta_i = \pi i/3 + w_i, \quad y_i = (\cos\theta_i, \sin\theta_i, 0) \quad (1 \leq i \leq 6),$$

where w_i is a uniform variate in the range $(-0.05\pi, +0.05\pi)$. The purpose of the $w_i's$ is to simulate the inaccuracy that arises when the CMM operator judges by eye that the points are evenly spaced around the circle.

Step 2, rotation matrices R_j $(1 \leq j \leq n)$ are selected with the property that $R_1 v_0$, $R_2 v_0$, $R_3 v_0$ are mutually orthogonal. Put

$$v_j = R_j v_0 \quad (1 \leq j \leq n).$$

The above orthogonality requirement is included to avoid the degenerate situation where all the normals are nearly in the same straight line.

Step 3, an arbitrary rotation R is applied to all the data. Then

$$u_j = R v_j \quad (1 \leq j \leq n)$$

are the 'true' CMM normals, and if we put

$$x_{ji} = R R_j y_i \quad (1 \leq j \leq n, 1 \leq i \leq 6),$$

the vectors $x_{j1}, x_{j2}, \ldots, x_{j6}$ are the CMM points that would be used to estimate u *via* the method of Section 2.

The above data simulates a part that is geometrically perfect, and has been measured without any error, *i.e.*, the CMM has $\epsilon = 0$. The algorithms of Sections 2 and 3 would lead to estimators

$$\hat{u}_j = u_j \quad (1 \leq j \leq n), \tag{4.5}$$

and a rotation matrix

$$A_{ls} = R. \tag{4.6}$$

A.1. Putting in Errors

Different scenarios are considered, by varying n and the resolution ϵ, of the CMM. The basic idea of the study is to simulate measurement errors on the CMM readings x_{ji} consistent with the error structure discussed in Section 2.1, so that the κ induced by the resolution of the CMM would be the allowable tolerance κ_0. By taking many iterations, κ would be estimated for each scenario. Once κ is estimated for parts that are geometrically perfect, the estimate $\hat{\kappa}$, would serve as the tolerance level, *i.e.*, $\kappa_0 = \hat{\kappa}$. We then simulate "defective" parts by displacing one or more CMM normals by some small angle ϕ. This is achieved by setting

$$x_{ji} = RR_j^{\phi} y_i \quad (1 \leq i \leq 6)$$

for one or more values of j, where R_j^{ϕ} is R_j composed with a rotation through an angle ϕ about an arbitrary axis. The diagnostics (3.16) and (3.17) can now be tested, for various angles ϕ.

ACKNOWLEDGEMENTS

The work presented in this paper arose in the development of the **Soft-Fit System**^{TM}. This is a complete quality assurance software system developed by TAVA Corporation (formerly Lexus Corporation) of London, Ontario. The first author wishes to thank TAVA personnel, in particular Brian McIlhargey and Bob Stone, for their enthusiasm, support and cooperation.

Part of the support for the research of the second author was provided by a grant from the Natural Sciences and Engineering Research Council of Canada. Further, part of the research was performed during a visit to the Mathematics Department at the University of Oregon.

Finally, both authors wish to thank Steve Gismondi, a mathematics graduate student at the University of Guelph, for providing assistance in programing and simulations. We would also like to thank Andrew Booker (Boeing), Ted Chang (Virginia), Louis-Paul Rivest (Laval) and Jeff Wu (Waterloo) for their discussions and suggestions.

REFERENCES

Bingham, C. and Chang, T. (1988). The use of the Bingham distribution in spherical regression inference. *School of Statistics, University of Minnesota*, Report **514**, May 1988.

Blow, D.M. (1960). To fit a plane to a set of points by least squares. *Acta Cryst*, **13**, 168.

Chang, T. (1986). Spherical regression. *Ann Statist*, **14**, 907-924.

Chang, T. (1989). Spherical regression with errors in variables. *Ann Statist*, **17**, 293-306.

Golub, G.H. and Van Loan, C.F. (1983). *Matrix Computations.* John Hopkins University Press, Baltimore, Maryland.

Kim, P.T. (1991). Decision theoretic analysis of spherical regression. *J Mult Analysis*, **38**, 233-240.

MacKenzie, J.K. (1957). The estimation of an orientation relationship. *Acta Cryst*, **10**, 61-62.

Moran, P.A.P. (1976). Quaternions, Haar measure and the estimation of a paleomagnetic rotation. In *Perspectives in Probability and Statistics*, Journal of Applied Probability Trust and Academic press, London 295-301.

Prentice, M.J. (1986). Orientation statistics without parametric assumptions. *JR Statist Soc B*, **51**, 214-222.

Rivest, L.P. (1989). Spherical regression for concentrated Fisher-von Mises distributions. *Ann Statist*, **17**, 307-317.

Scheringer, C. (1971). A method of fitting a plane to a set of points by least squares. *Acta Cryst*, B **27**, 1470-1472.

Schomaker, V., J. Waser, R.E. Marsh and G. Bergman (1959). To fit a plane or a line to a set of points by least squares. *Acta Cryst*, **12**, 600-604.

Stephens, M.A. (1979). Vector correlation. *Biometrika*, **66**, 41-48.

Figure 3.1. Orientation of spatial bodies

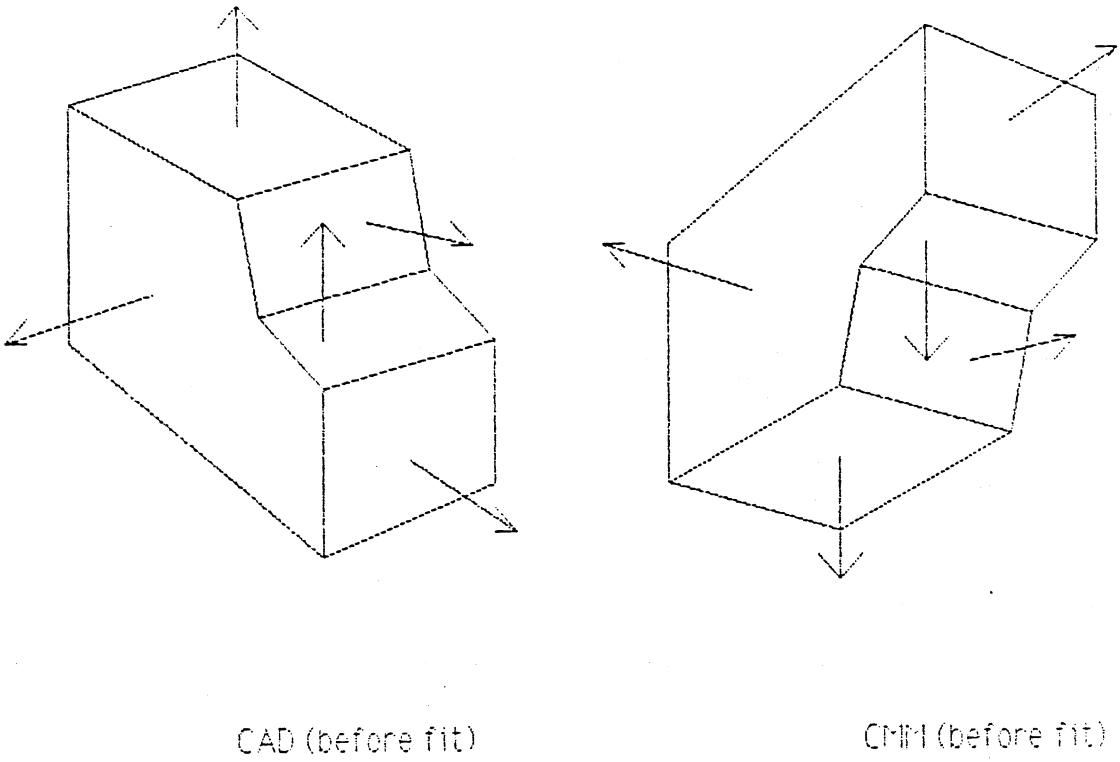

Figure 4.1. Graph of $\ln(\hat{\kappa})$ versus CMM resolution, ϵ, for $n = 10$

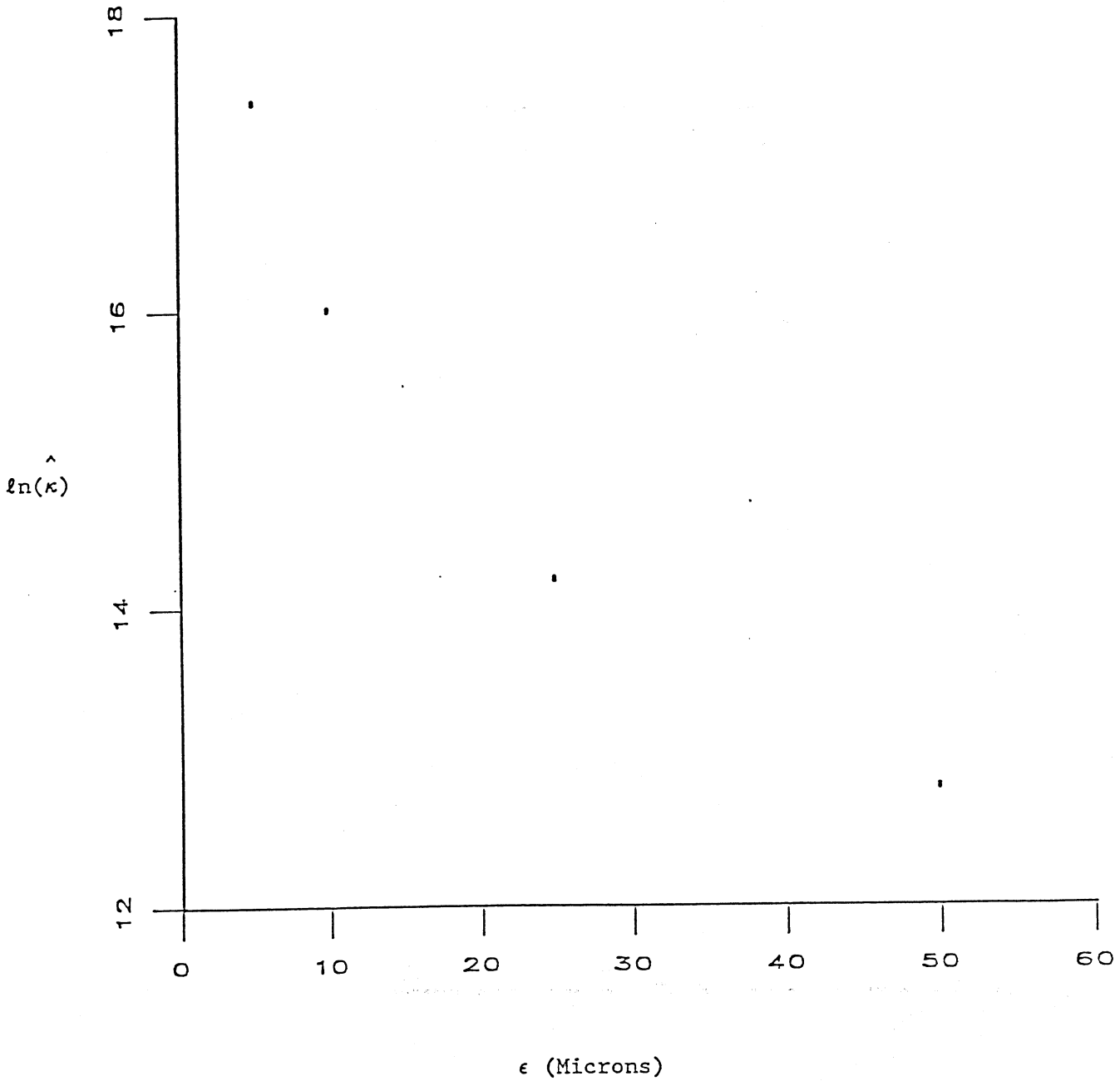

Table 5.1. Number of parts rejected in 100 trials, using criterion (5.1), with number of normals (a) $n = 3$, (b) $n = 10$. One normal is displaced ϕ radians, and ϵ (microns) denotes machine resolution.

(a) n=3

		ϕ (radians)				
		0	0.001	0.002	0.005	0.010
ϵ (microns)	5	7	97	100	100	100
	10	2	34	97	100	100
	25	3	9	31	95	100
	50	9	9	13	46	96

(b) n=10

		ϕ (radians)				
		0	0.001	0.002	0.005	0.010
ϵ (microns)	5	5	99	100	100	100
	10	5	27	95	100	100
	25	4	10	20	97	100
	50	5	6	4	32	99

Table 5.2. Number of parts rejected in 100 trials, using criterion (5.2), with number of normals (a) $n = 3$, (b) $n = 10$. One normal is displaced ϕ radians, and ϵ (microns) denotes machine resolution.

(a) n=3

		ϕ (radians)				
		0	0.001	0.002	0.005	0.010
ϵ (microns)	5	2	21	33	80	95
	10	4	9	25	44	66
	25	8	10	12	22	33
	50	8	8	4	9	10

(b) n=10

		ϕ (radians)				
		0	0.001	0.002	0.005	0.010
ϵ (microns)	5	4	100	100	100	100
	10	3	66	100	100	100
	25	4	12	41	100	100
	50	2	2	12	59	100

Table 5.3. Number of parts rejected in 100 trials, using criterion (5.2), with number of normals (a) $n = 3$, (b) $n = 10$. One normal is displaced ϕ radians, and ϵ (microns) denotes machine resolution.

(a) n=3

		ϕ (radians)				
		0	0.001	0.002	0.005	0.010
ϵ (microns)	5	13	0	0	0	0
	10	9	4	0	0	0
	25	12	7	4	1	0
	50	9	10	8	5	0

(b) n=10

		ϕ (radians)				
		0	0.001	0.002	0.005	0.010
ϵ (microns)	5	34	1	0	0	0
	10	30	13	1	0	0
	25	37	30	15	0	0
	50	36	43	25	7	0

Table 5.4. Number of parts rejected in 100 trials, using criterion (5.1), with number of normals (a) $n = 3$, (b) $n = 10$. Three normals are displaced ϕ radians, and ϵ (microns) denotes machine resolution.

(a) n=3

		ϕ (radians)				
		0	0.001	0.002	0.005	0.010
ϵ (microns)	5	8	100	100	100	100
	10	1	72	100	100	100
	25	6	13	45	100	100
	50	3	9	26	69	100

(b) n=10

		ϕ (radians)				
		0	0.001	0.002	0.005	0.010
ϵ (microns)	5	4	100	100	100	100
	10	7	86	100	100	100
	25	5	17	55	100	100
	50	2	8	10	87	100

Table 5.5. Number of parts rejected in 100 trials, using criterion (5.2), with number of normals (a) $n = 3$, (b) $n = 10$. Three normals are displaced ϕ radians, and ϵ (microns) denotes machine resolution.

(a) n=3

		ϕ (radians)				
		0	0.001	0.002	0.005	0.010
ϵ (microns)	4	8	39	71	98	100
	10	12	29	47	83	96
	25	10	13	14	43	70
	50	10	18	13	21	38

(b) n=10

		ϕ (radians)				
		0	0.001	0.002	0.005	0.010
ϵ (microns)	5	11	72	79	90	100
	10	8	53	62	84	95
	25	13	18	46	66	79
	50	13	19	22	50	78